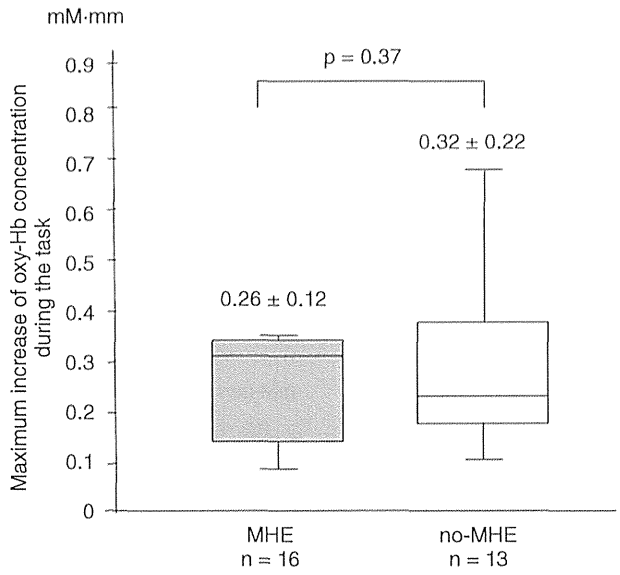

Figure 4 Comparison of maximum increase in oxygenated hemoglobin (oxy-Hb) concentration between patients with and without minimal hepatic encephalopathy (MHE). The average value of maximum increase in oxy-Hb did not differ significantly between the MHE and non-MHE groups.

0.11 ± 0.09 mM · mm, $P = 0.006$) (Fig. 5). For the diagnosis of MHE, the receiver–operator curve analysis identified an optimal cut-off of 0.05 mM · mm for the oxy-Hb concentration at 5 s after starting the task. The area under the curve was 0.774 ($P = 0.012$; 95% confidence interval, 0.60–0.95), sensitivity and specificity of NIRS for the diagnosis of MHE was 69% and 77%, respectively. The positive predictive value was 79% and negative predictive value was 67%.

DISCUSSION

USING NIRS, WHICH can detect changes in regional cerebral oxy-Hb concentration with an extremely high level of sensitivity, we found that increase in cerebral oxy-Hb concentration in response to tasks was slow and small among cirrhotic patients without OHE but having abnormal electroencephalography findings. The impairment of response was most significant at an early time point after the start of the task. These findings indicated that cerebral oxygen metabolism is poorly reactive in response to tasks among patients with MHE and that this impaired cerebral oxygen metabolism may be related to the pathogenesis of latent impairment of brain activity seen in MHE. To the best of our knowledge, our study appears to be the first evaluating MHE with NIRS. The non-invasiveness and high time resolution of NIRS give it potential as a valuable research tool for the examination of brain function in HE, as well as a clinically useful tool for the diagnosis of MHE.

Hepatic encephalopathy in its early stage, such as latent or minimal HE, can reduce cognitive function, lower work efficiency, reduce QOL[27,28] or impair driving skill.[1,2,29,30] Although there are several practical requirements for the diagnosis of MHE, adequate diagnosis of MHE is difficult due to the lack of reliable diagnostic standards.[31,32] Several diagnostic methods such as neuropsychological function tests, number connection test, light/sound reaction time, inhibitory control test, WAIS or electro-psychological tests including EEG, spectral EEG, and cerebral evoked potential, PHES, critical flicker test and computer-aided quantitative neuropsychological function test system (NP-test)[7–15] have been proposed,[32–36] but there is no ideal test for MHE as yet. Because these tests are developed for the screening of MHE, these are not diagnostic. Establishment of a reliable diagnostic method for MHE is imperative. We

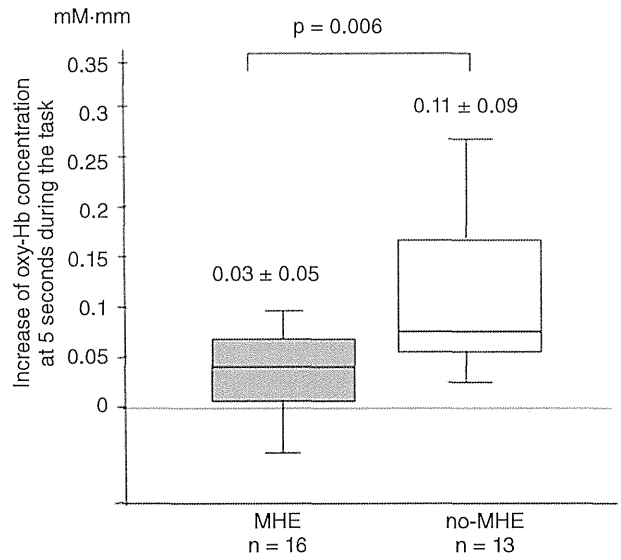

Figure 5 Comparison of increase in oxygenated hemoglobin (oxy-Hb) concentration at 5 s after the start of task between patients with and without minimal hepatic encephalopathy (MHE). The average value of increase in oxy-Hb was compared between the MHE and non-MHE groups at 5 s after starting the word-fluency task. The increase in the oxy-Hb concentration was significantly lower in patients with MHE compared to non-MHE ($P = 0.006$).

have some cases in which NIRS results improved with lactulose and branched-chain amino acid. A prospective study is ongoing to evaluate the effect of treatment by NIRS. The major advantage of NIRS over "paper and pencil tests" is the absence of learning effect which is generally seen in other neuropsychological function tests[37] and NIRS could also discriminate other mental disorders.[24,25]

Neuroimaging using MRI, magnetic resonance spectroscopy and PET has made it possible to non-invasively assess hepatic encephalopathy.[38–47] However, these tests require extensive equipment and are therefore costly. NIRS is a new methodology for brain research and brain function testing, and has applications in various areas of medicine, being used not only in research, but also in clinical medicine.[23–25,48] NIRS has been approved for identifying the language-dominant hemisphere before brain surgery and measuring epileptic foci.[49] In human studies comparing NIRS and fMRI,[50–52] a correlation was seen between blood-oxygen-level-dependent signal and oxy-Hb concentration as measured by NIRS. In brain function analysis, the detection sensitivity of NIRS is comparable to that of fMRI, but the time resolution of NIRS is greater. Furthermore, the advantages of NIRS are convenience, bedside analysis, non-invasiveness, free task setting and low cost.

Here, we used multichannel NIRS to measure the changes in oxy-Hb concentration during task performance from the frontal to temporal regions of the cortex in MHE patients and compared the results with those of liver cirrhosis without MHE. In all subjects, oxy-Hb increased during task performance and gradually decreased after the completion of task performance. However, the time-dependent changes in the degree of increase in oxy-Hb concentration differed between patients with and without MHE. The degree of increase in oxy-Hb concentration during task performance was smaller and more gradual in MHE compared to non-MHE patients. The increase of the oxy-Hb concentration reflects the increase of cerebral blood volume in the area of the brain activated by the task. Iversen *et al.* found that the cerebral oxygen consumption and blood flow were both reduced in cirrhotic patients with an acute episode of OHE[16]and that the oxygen delivery was approximately twice the oxygen consumption, indicating that oxygen delivery or blood flow was not a limiting factor for the oxygen consumption. Consequently, cerebral blood flow seems to be reduced as a result of diminished cerebral oxygen requirement during HE, and not vice versa.[16] It is reported that neuron-to-astrocyte signaling is a key mechanism in functional hyperemia,[17–19,53,54] and that function of astrocytes is impaired in hepatic encephalopathy patients.[20–22] Therefore, impaired astrocyte-mediated control of cerebral microcirculation can result in slow increase of cerebral blood flow during task performance in MHE patients. Thus, the sluggish increase in cerebral blood flow seen in MHE in the present study may reflect the impaired brain activity and dysfunction of astrocytes and impaired cerebral oxygen metabolism in these patients.

There are several limitations in the present study. The number of patients was not enough to make a comparison stratified by Child grade. We would like to analyze this important point in a future study. It may be possible that cerebral oxy-Hb may change due to aging or by the arteriosclerotic changes. In the present study, age was not related to NIRS results. All patients were examined by brain MRI or brain CT and they had no apparent brain structural disease including brain infarction. However, it was not possible to evaluate the arteriosclerotic changes. This may be another limitation of this study. Many neuropsychological function tests, such as number connection test, light/sound reaction time, inhibitory control test, WAIS or electro-psychological tests including EEG, cerebral evoked potential, p300 event-related potential, PHES and critical flicker test have been employed for the diagnosis of MHE. In Japan, Kato and colleagues established the computer-aided quantitative neuropsychological function test system called NP-test.[7] However, these tests were not simultaneously measured in the present study. Because we recognize the importance of comparing NIRS with other tests, we would like to solve this issue in future study.

In conclusion, NIRS, with its high degree of time resolution, enabled us to identify the characteristic time course of oxy-Hb concentration changes during tasks in MHE. The observations imply that cerebral oxygen supply and metabolism is poorly reactive in MHE, which may be related to the pathogenesis of latent impairment of brain activity.

REFERENCES

1 Bajaj JS, Hafeezullah M, Hoffmann RG *et al.* Navigation skill impairment: another dimension of the driving difficulties in minimal hepatic encephalopathy. *Hepatology* 2008; **47**: 596–604.
2 Bajaj JS, Pinkerton SD, Sanyal AJ, Heuman DM. Diagnosis and treatment of minimal hepatic encephalopathy to prevent motor vehicle accidents: a cost-effectiveness analysis. *Hepatology* 2012; **55**: 1164–71.

3 Dhiman RK, Kurmi R, Thumburu KK *et al.* Diagnosis and prognostic significance of minimal hepatic encephalopathy in patients with cirrhosis of liver. *Dig Dis Sci* 2010; **55**: 2381–90.
4 Bajaj JS, Heuman DM, Wade JB *et al.* Rifaximin improves driving simulator performance in a randomized trial of patients with minimal hepatic encephalopathy. *Gastroenterology* 2011; **140**: 478–87 e1.
5 Prasad S, Dhiman RK, Duseja A, Chawla YK, Sharma A, Agarwal R. Lactulose improves cognitive functions and health-related quality of life in patients with cirrhosis who have minimal hepatic encephalopathy. *Hepatology* 2007; **45**: 549–59.
6 Sharma P, Sharma BC, Agrawal A, Sarin SK. Primary prophylaxis of overt hepatic encephalopathy in patients with cirrhosis: an open labeled randomized controlled trial of lactulose versus no lactulose. *J Gastroenterol Hepatol* 2012; **27**: 1329–35.
7 Kato A, Watanabe Y, Sawara K, Suzuki K. Diagnosis of sub-clinical hepatic encephalopathy by Neuropsychological Tests (NP-tests). *Hepatol Res* 2008; **38** (Suppl 1): S122–7.
8 Kircheis G, Wettstein M, Timmermann L, Schnitzler A, Haussinger D. Critical flicker frequency for quantification of low-grade hepatic encephalopathy. *Hepatology* 2002; **35**: 357–66.
9 Romero-Gomez M, Cordoba J, Jover R *et al.* Value of the critical flicker frequency in patients with minimal hepatic encephalopathy. *Hepatology* 2007; **45**: 879–85.
10 Amodio P, Campagna F, Olianas S *et al.* Detection of minimal hepatic encephalopathy: normalization and optimization of the Psychometric Hepatic Encephalopathy Score. A neuropsychological and quantified EEG study. *J Hepatol* 2008; **49**: 346–53.
11 Davies MG, Rowan MJ, MacMathuna P, Keeling PW, Weir DG, Feely J. The auditory P300 event-related potential: an objective marker of the encephalopathy of chronic liver disease. *Hepatology* 1990; **12**: 688–94.
12 Kugler CF, Lotterer E, Petter J *et al.* Visual event-related P300 potentials in early portosystemic encephalopathy. *Gastroenterology* 1992; **103**: 302–10.
13 Bajaj JS, Hafeezullah M, Franco J *et al.* Inhibitory control test for the diagnosis of minimal hepatic encephalopathy. *Gastroenterology* 2008; **135**: 1591–600 e1.
14 Sharma P, Kumar A, Singh S, Tyagi P. Inhibitory control test, critical flicker frequency, and psychometric tests in the diagnosis of minimal hepatic encephalopathy in cirrhosis. *Saudi J Gastroenterol* 2013; **19**: 40–4.
15 Goldbecker A, Weissenborn K, Hamidi Shahrezaei G *et al.* Comparison of the most favoured methods for the diagnosis of hepatic encephalopathy in liver transplantation candidates. *Gut* 2013. doi: 10.1136/gutjnl-2012-303262.
16 Iversen P, Sorensen M, Bak LK *et al.* Low cerebral oxygen consumption and blood flow in patients with cirrhosis and an acute episode of hepatic encephalopathy. *Gastroenterology* 2009; **136**: 863–71.
17 Gordon GR, Choi HB, Rungta RL, Ellis-Davies GC, MacVicar BA. Brain metabolism dictates the polarity of astrocyte control over arterioles. *Nature* 2008; **456**: 745–9.
18 Takano T, Tian GF, Peng W *et al.* Astrocyte-mediated control of cerebral blood flow. *Nat Neurosci* 2006; **9**: 260–7.
19 Magistretti PJ. Neuron-glia metabolic coupling and plasticity. *J Exp Biol* 2006; **209**: 2304–11.
20 Gorg B, Qvartskhava N, Keitel V *et al.* Ammonia induces RNA oxidation in cultured astrocytes and brain in vivo. *Hepatology* 2008; **48**: 567–79.
21 Albrecht J, Norenberg MD. Glutamine: a Trojan horse in ammonia neurotoxicity. *Hepatology* 2006; **44**: 788–94.
22 Lemberg A, Fernandez MA. Hepatic encephalopathy, ammonia, glutamate, glutamine and oxidative stress. *Ann Hepatol* 2009; **8**: 95–102.
23 Maki A, Yamashita Y, Ito Y, Watanabe E, Mayanagi Y, Koizumi H. Spatial and temporal analysis of human motor activity using noninvasive NIR topography. *Med Phys* 1995; **22**: 1997–2005.
24 Kameyama M, Fukuda M, Yamagishi Y *et al.* Frontal lobe function in bipolar disorder: a multichannel near-infrared spectroscopy study. *Neuroimage* 2006; **29**: 172–84.
25 Suto T, Fukuda M, Ito M, Uehara T, Mikuni M. Multichannel near-infrared spectroscopy in depression and schizophrenia: cognitive brain activation study. *Biol Psychiatry* 2004; **55**: 501–11.
26 Takizawa R, Kasai K, Kawakubo Y *et al.* Reduced frontopolar activation during verbal fluency task in schizophrenia: a multi-channel near-infrared spectroscopy study. *Schizophr Res* 2008; **99**: 250–62.
27 Groeneweg M, Quero JC, De Bruijn I *et al.* Subclinical hepatic encephalopathy impairs daily functioning. *Hepatology* 1998; **28**: 45–9.
28 Marchesini G, Bianchi G, Amodio P *et al.* Factors associated with poor health-related quality of life of patients with cirrhosis. *Gastroenterology* 2001; **120**: 170–8.
29 Schomerus H, Hamster W, Blunck H, Reinhard U, Mayer K, Dolle W. Latent portasystemic encephalopathy. I. Nature of cerebral functional defects and their effect on fitness to drive. *Dig Dis Sci* 1981; **26**: 622–30.
30 Wein C, Koch H, Popp B, Oehler G, Schauder P. Minimal hepatic encephalopathy impairs fitness to drive. *Hepatology* 2004; **39**: 739–45.
31 Ferenci P, Lockwood A, Mullen K, Tarter R, Weissenborn K, Blei AT. Hepatic encephalopathy – definition, nomenclature, diagnosis, and quantification: final report of the working party at the 11th World Congresses of Gastroenterology, Vienna, 1998. *Hepatology* 2002; **35**: 716–21.
32 Ortiz M, Jacas C, Cordoba J. Minimal hepatic encephalopathy: diagnosis, clinical significance and recommendations. *J Hepatol* 2005; **42** (Suppl): S45–53.
33 Niedermeyer E. The clinical relevance of EEG interpretation. *Clin Electroencephalogr* 2003; **34**: 93–8.

34 Amodio P, Pellegrini A, Ubiali E *et al.* The EEG assessment of low-grade hepatic encephalopathy: comparison of an artificial neural network-expert system (ANNES) based evaluation with visual EEG readings and EEG spectral analysis. *Clin Neurophysiol* 2006; **117**: 2243–51.
35 Amodio P, Marchetti P, Del Piccolo F *et al.* Spectral versus visual EEG analysis in mild hepatic encephalopathy. *Clin Neurophysiol* 1999; **110**: 1334–44.
36 Sagales T, Gimeno V, de la Calzada MD, Casellas F, Dolors Macia M, Villar Soriano M. Brain mapping analysis in patients with hepatic encephalopathy. *Brain Topogr* 1990; **2**: 221–8.
37 Bajaj JS, Cordoba J, Mullen KD *et al.* Review article: the design of clinical trials in hepatic encephalopathy – an International Society for Hepatic Encephalopathy and Nitrogen Metabolism (ISHEN) consensus statement. *Aliment Pharmacol Ther* 2011; **33**: 739–47.
38 Ross BD, Danielsen ER, Bluml S. Proton magnetic resonance spectroscopy: the new gold standard for diagnosis of clinical and subclinical hepatic encephalopathy? *Dig Dis* 1996; **14** (Suppl 1): 30–9.
39 Ross BD, Jacobson S, Villamil F *et al.* Subclinical hepatic encephalopathy: proton MR spectroscopic abnormalities. *Radiology* 1994; **193**: 457–63.
40 Minguez B, Garcia-Pagan JC, Bosch J *et al.* Noncirrhotic portal vein thrombosis exhibits neuropsychological and MR changes consistent with minimal hepatic encephalopathy. *Hepatology* 2006; **43**: 707–14.
41 Kato A, Suzuki K, Kaneta H, Obara H, Fujishima Y, Sato S. Regional differences in cerebral glucose metabolism in cirrhotic patients with subclinical hepatic encephalopathy using positron emission tomography. *Hepatol Res* 2000; **17**: 237–45.
42 Taylor-Robinson SD, Sargentoni J, Mallalieu RJ *et al.* Cerebral phosphorus-31 magnetic resonance spectroscopy in patients with chronic hepatic encephalopathy. *Hepatology* 1994; **20**: 1173–8.
43 Laubenberger J, Haussinger D, Bayer S, Gufler H, Hennig J, Langer M. Proton magnetic resonance spectroscopy of the brain in symptomatic and asymptomatic patients with liver cirrhosis. *Gastroenterology* 1997; **112**: 1610–6.
44 Kale RA, Gupta RK, Saraswat VA *et al.* Demonstration of interstitial cerebral edema with diffusion tensor MR imaging in type C hepatic encephalopathy. *Hepatology* 2006; **43**: 698–706.
45 Lockwood AH, Yap EW, Rhoades HM, Wong WH. Altered cerebral blood flow and glucose metabolism in patients with liver disease and minimal encephalopathy. *J Cereb Blood Flow Metab* 1991; **11**: 331–6.
46 Lockwood AH. Positron emission tomography in the study of hepatic encephalopathy. *Metab Brain Dis* 2002; **17**: 431–5.
47 Ahl B, Weissenborn K, van den Hoff J *et al.* Regional differences in cerebral blood flow and cerebral ammonia metabolism in patients with cirrhosis. *Hepatology* 2004; **40**: 73–9.
48 Cyranoski D. Neuroscience: thought experiment. *Nature* 2011; **469**: 148–9.
49 Watanabe E, Nagahori Y, Mayanagi Y. Focus diagnosis of epilepsy using near-infrared spectroscopy. *Epilepsia* 2002; **43** (Suppl 9): 50–5.
50 Strangman G, Culver JP, Thompson JH, Boas DA. A quantitative comparison of simultaneous BOLD fMRI and NIRS recordings during functional brain activation. *Neuroimage* 2002; **17**: 719–31.
51 Sassaroli A, deB Frederick B, Tong Y, Renshaw PF, Fantini S. Spatially weighted BOLD signal for comparison of functional magnetic resonance imaging and near-infrared imaging of the brain. *Neuroimage* 2006; **33**: 505–14.
52 Huppert TJ, Hoge RD, Diamond SG, Franceschini MA, Boas DA. A temporal comparison of BOLD, ASL, and NIRS hemodynamic responses to motor stimuli in adult humans. *Neuroimage* 2006; **29**: 368–82.
53 Zonta M, Angulo MC, Gobbo S *et al.* Neuron-to-astrocyte signaling is central to the dynamic control of brain microcirculation. *Nat Neurosci* 2003; **6**: 43–50.
54 Schummers J, Yu H, Sur M. Tuned responses of astrocytes and their influence on hemodynamic signals in the visual cortex. *Science* 2008; **320**: 1638–43.

Hepatology Research

Hepatology Research 2014; 44: 1339–1346 doi: 10.1111/hepr.12309

Original Article

Hepatocellular carcinoma risk assessment using gadoxetic acid-enhanced hepatocyte phase magnetic resonance imaging

Nobutoshi Komatsu,[1] Utaroh Motosugi,[2] Shinya Maekawa,[1] Kuniaki Shindo,[1] Minoru Sakamoto,[1] Mitsuaki Sato,[1] Akihisa Tatsumi,[1] Mika Miura,[1] Fumitake Amemiya,[1] Yasuhiro Nakayama,[1] Taisuke Inoue,[1] Mitsuharu Fukasawa,[1] Tomoyoshi Uetake,[1] Masahiko Ohtaka,[1] Tadashi Sato,[1] Yasuhiro Asahina,[3] Masayuki Kurosaki,[4] Namiki Izumi,[4] Tomoaki Ichikawa,[2] Tsutomu Araki[2] and Nobuyuki Enomoto[1]

[1]*First Department of Internal Medicine,* [2]*Department of Radiology, University of Yamanashi, Yamanashi,* [3]*Department of Gastroenterology and Hepatology, Tokyo Medical and Dental University, and* [4]*Department of Gastroenterology and Hepatology, Musashino Red Cross Hospital, Tokyo, Japan*

Aim: To investigate whether the patients with hypovascular liver nodules determined on the arterial phase and hypointensity on the hepatocyte phase gadoxetic acid-enhanced magnetic resonance imaging (hypovascular hypointense nodules) are at increased risk of hepatocarcinogenesis, we assessed subsequent typical hepatocellular carcinoma (HCC) development at any sites of the liver with and without such nodules.

Methods: One hundred and twenty-seven patients with chronic hepatitis B or C and without a history of HCC, including 68 with liver cirrhosis, were divided into those with (non-clean liver group, $n = 18$) and without (clean liver group, $n = 109$) hypovascular hypointense nodules. All the patients were followed up for 3 years, and HCC development rates and risk factors were analyzed with the Kaplan–Meier method and the Cox proportional hazard model, respectively.

Results: A total of 17 patients (10 in the non-clean liver group and seven in the clean liver group) developed typical HCC. Cumulative 3-year rates of HCC development were 55.5% in the non-clean liver group and 6.4% in the clean liver group ($P < 0.001$), and those at the different sites from the initial nodules was also higher in the non-clean liver group (22.2%) than the clean liver group (6.4%) ($P = 0.003$). Multivariate analysis identified older age ($P = 0.024$), low platelet counts ($P = 0.017$) and a non-clean liver ($P < 0.001$) as independent risk factors for subsequent HCC development.

Conclusion: Patients with hypovascular hypointense liver nodules are at a higher risk for HCC development at any sites of the liver than those without such nodules.

Key words: gadoxetic acid, hepatocellular carcinoma, hepatocyte phase, magnetic resonance imaging, risk assessment

INTRODUCTION

HEPATOCELLULAR CARCINOMA (HCC) is one of the most common cancers worldwide and is a major cause of death in patients with chronic viral liver disease. Despite many advances in multidisciplinary treatment, complete curative treatment of early stage HCC remains the only possible therapeutic choice for long-term survival. Therefore, surveillance programs for patients at a high risk for HCC that include imaging-based evaluations are crucial for the detection and treatment of early stage HCC.

The newly introduced magnetic resonance imaging (MRI) contrast agent, gadolinium ethoxybenzyl

Correspondence: Dr Nobuyuki Enomoto, First Department of Internal Medicine, University of Yamanashi, 1110 Shimokato, Chuo, Yamanashi 409-3898, Japan. Email: enomoto@yamanashi.ac.jp

Conflict of interest: All authors have no conflict of interest related to this manuscript.

Funding: This study was supported in part by a Grant-in-Aid from the Ministry of Education, Science, Sports and Culture of Japan (23390195, 23791404, 24590964 and 24590965), and in part by a Grant-in-Aid from the Ministry of Health, Labor and Welfare of Japan (H23-kanen-001, H23-kanen-004, H23-kanen-006, H24-kanen-002, H24-kanen-004 and H25-kanen-006).

Received 18 August 2013; revision 13 January 2014; accepted 28 January 2014.

diethylenetriamine pentaacetic acid (gadoxetic acid), has enabled concurrent assessment of tumor vascularity and unique hepatocyte-specific contrast (hepatocyte phase).[1–3] This has led to the frequent identification of hypovascular nodules determined on the arterial phase with hypointensity on the hepatocyte phase (hypovascular hypointense nodules),[4–8] while many of these nodules are difficult to be detected by ultrasonography (US) or computed tomography (CT). Recently, the natural history of hypovascular hypointense nodules themselves were reported in several studies,[9–12] revealing the high risk of subsequent progress to typical HCC from these nodules. However, it is not well known whether patients with such nodules have a higher risk of developing typical HCC at any sites of the liver, including at the different sites from initial nodules, compared to those without such nodules.

If patients with these nodules may have a high risk of developing typical HCC not only at the same sites but also at the different sites from initial nodules, a significant proportion of these nodules are precancerous lesions or early stage HCC as reported,[13–15] and more importantly, the liver with these nodules may reflect a higher potential for hepatocarcinogenesis or the presence of undetectable precursor lesions in other sites of the liver. Conversely, the absence of these nodules potentially identifies the patients at a low risk for subsequent typical HCC development at any sites. The purpose of this study was to assess the risk of subsequent typical HCC development at any sites of the liver with and without hypovascular hypointense nodules on gadoxetic acid-enhanced MRI.

METHODS

Ethical review

THE PROTOCOL OF this retrospective study was approved by the ethics committee of Yamanashi University Hospital, which waived the requirement for written informed consent because the study was a retrospective data analysis, with appropriate consideration given to patient risk, privacy, welfare and rights.

Patients

We recruited 559 consecutive outpatients with chronic hepatitis B virus (HBV) or hepatitis C virus (HCV) infection who underwent gadoxetic acid-enhanced MRI at Yamanashi University Hospital between January 2008 and December 2010. The exclusion criteria were as follows: (i) presence or history of typical HCC ($n = 420$), because intrahepatic metastasis does not always develop through the usual multistep hepatocarcinogenesis process, skipping the early pathological stage with hypovascularity to an advanced pathological stage even when the size is small;[16,17] (ii) Child–Pugh class C disease ($n = 9$), because the hepatocyte phase findings are not reliable in patients with this condition because of reduced gadoxetic acid uptake in the liver;[18] and (iii) patients who dropped out during the 3-year follow-up period ($n = 3$).

After excluding 432 patients, 127 patients were included in this retrospective cohort study. They were divided into groups with hypovascular nodules determined on the arterial phase and hypointensity on the hepatocyte phase (non-clean liver group; $n = 18$ patients) and without such nodules (clean liver group; $n = 109$ patients) as shown in Figure 1. In this study, we divided cases into two groups according to the presence or absence of these nodules at the baseline, even when such nodules were initially detected during the follow-up period; we assigned these patients to the clean liver group.

Follow up and diagnosis of HCC

All 127 patients were followed up at the liver disease outpatient clinic of our institution with blood tests, including those for tumor markers and diagnostic imaging modality (US, CT or MRI). The development of typical HCC that required treatment as proposed by the American Association for the Study of Liver Diseases (AASLD) guidelines[19] and that was diagnosed according to imaging criteria, showing arterial hypervascularity and venous phase washout, or based on histological examination of liver biopsies from hypovascular nodules that grew to more than 10 mm during follow up. Biopsies were obtained using a 21-G core needle. Two patients each had a liver nodule of more than 10 mm in diameter on initial MRI (12 mm and 13 mm), which were diagnosed on the basis of the biopsy as dysplastic nodules.

The end-point of this study was the development of typical HCC not only from the hypovascular hypointense nodules observed initially but also from other areas without these nodules ("de novo HCC"). Dynamic CT and/or MRI were also performed in cases with hepatic nodules detected by US, liver cirrhosis, a tendency of tumor marker elevation and difficult evaluation of the liver parenchyma by US. All 127 patients were followed up for 3 years after the initial gadoxetic acid-enhanced MRI examination. When imaging

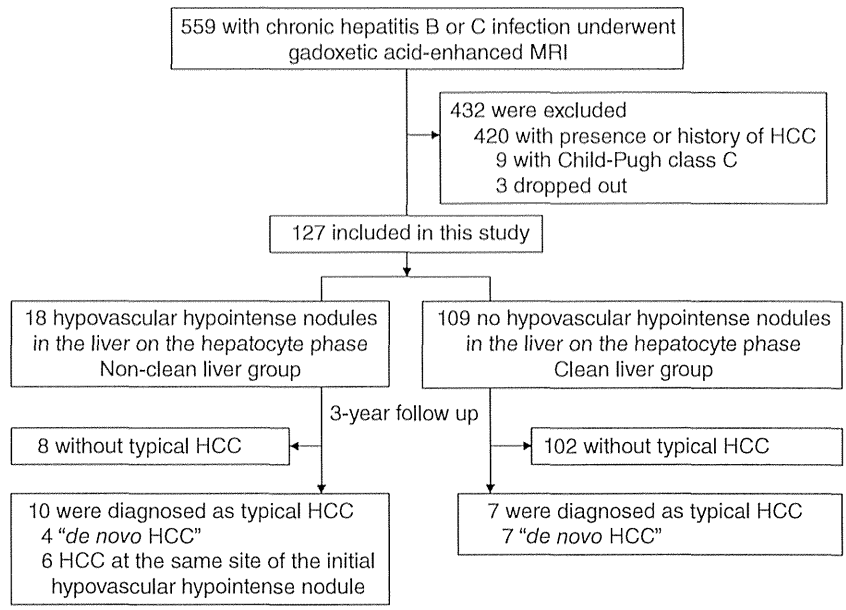

Figure 1 Patient inclusion criteria. "De novo HCC" is a typical hepatocellular carcinoma that developed at sites in which no nodules had been seen on the initial gadoxetic acid-enhanced magnetic resonance imaging (MRI).

modalities led to diagnosis of HCC, recognizing hypervascularization by more than one experienced radiologist and other imaging modalities was regarded as the time of diagnosis of HCC. When needle biopsy was performed to investigate nodules, the time of diagnosis of HCC was when the pathologists and physicians examined pathological tissue and diagnosed as HCC.

MRI

Magnetic resonance imaging was performed using a superconducting magnet that operated at 1.5 Tesla (Sigma EXCITE HD; GE Medical Systems, Milwaukee, WI, USA) and an 8-channel phased-array coil. First, we obtained fast spoiled gradient-echo T_1-weighted images (T1WI) with dual echo acquisition and respiratory-triggered fat-saturated fast spin-echo T_2-weighted images (T2WI). Dynamic fat-suppressed gradient-echo T1WI were obtained using a 3-D acquisition sequence before (precontrast) and 20–30 s, 60 s, 2 min, 5 min, 10 min and 20 min after the administration of gadoxetic acid (Primovist; Bayer Schering Pharma, Berlin, Germany). This contrast agent (0.025 mM/kg bodyweight) was administrated i.v. as a bolus at a rate of 1 mL/s through an i.v. cubital line (20–22 G) that was flushed with 20 mL saline from a power injector. The delay time for the arterial phase scan was adjusted according to a fluoroscopic triggering method.[20] All images were acquired in the transverse plane. Sagittal plane T1WI were also obtained during the hepatocyte phase at 20 min after the injection of the contrast agent.

Statistical analysis

All continuous values are expressed as median (range). Fisher's exact probability test was used for comparisons between categorical variable and the non-parametric Mann-Whitney *U*-test was used to compare differences between continuous variables. Baseline clinical characteristics, including blood test results, were evaluated within 1 month of the initial MRI. We investigated whether or not HCC development was associated with age, sex, fibrosis, etiology (HBV or HCV), platelet count, serum alanine aminotransferase (ALT), γ-glutamyltransferase (γ-GT), α-fetoprotein (AFP), and the presence or absence of hypovascular hypointense nodules.

Cumulative HCC development was estimated according to the Kaplan–Meier method and differences in the curves were tested using the log–rank test. Risk factors for HCC development were determined according to the Cox proportional hazard model. Subgroup analyses with a Cox proportional hazard model were applied to estimation of the hazard ratio (HR) of the non-clean liver group versus clean liver group in the dichotomized subgroups. All statistical analyses were performed using JMP software, version 10 (SAS Institute Japan, Tokyo, Japan). A two-sided *P*-value of less than 0.05 was considered statistically significant.

RESULTS

Characteristics of the patients and nodules

A TOTAL OF 127 patients were enrolled, of whom 26 had chronic HBV infections and 101 had HCV infections, and 68 had virus-associated cirrhosis. No statistically significant differences in the initial clinical characteristics were found between the non-clean liver and clean liver groups (Table 1). Thirty-five hypovascular hypointense nodules were found in 18 patients in the non-clean liver group (1–5 nodules per patient) at baseline (data not shown). Twenty-four of these 35 nodules were detectable only on the hepatocyte phase MRI and were undetectable by US, CT and non-hepatocyte phase MRI. None of the 35 nodules showed high intensity on T2WI. The median nodule diameter was 8 mm (range, 4–13 mm; 33 nodules with ≤10 mm, two nodules with 12 mm and 13 mm).

HCC incidence according to initial MRI findings

Hepatocellular carcinoma was diagnosed in 17 patients, 10 in the non-clean liver group and seven in the clean liver group; 14 of these patients had HCV infection. Thirteen patients were diagnosed according to the AASLD imaging criteria.[19] Four patients were diagnosed pathologically by liver biopsies that were performed, based on enlargement of the nodules of more than 10 mm in diameter during the observation period.

The cumulative 1-, 2- and 3-year HCC incidence rates were 1.5%, 10.2% and 13.4%, respectively. As determined by the Kaplan–Meier method, these rates were 11.1% (95% confidence interval [CI], 0.0–25.6%), 38.8% (95% CI, 16.3–61.4%) and 55.5% (95% CI, 32.6–78.5%) in the non-clean liver group, and 0.0% (95% CI, 0.0–2.3%), 5.5% (95% CI, 0.0–9.8%) and 6.4% (95% CI, 1.8–11.0%) in the clean liver group; the former group showed significantly higher rates of development of typical HCC than the latter ($P < 0.001$) as shown in Figure 2. The median imaging intervals were 3 months (range, 3–6) in the non-clean liver group and 4 months (range, 2–12) in the clean liver group. The imaging interval of the non-clean liver group was shorter than the clean liver group (3 vs 4 months, $P = 0.015$). The median intervals between the initial MRI and HCC diagnosis was 16 months (range, 9–32) in the non-clean liver group and 21 months (range, 16–35) in the clean liver group.

In 11 of 17 patients with HCC development, HCC developed at sites in which no nodules had been seen on the initial gadoxetic acid-enhanced MRI, namely de novo HCC. These HCC were found in four of 18 patients in the non-clean liver group (3-year HCC incidence rates: 22.2%; 95% CI, 4.3–51.0%) and 7 in 109 patients in the clean liver group (3-year HCC incidence rates: 6.4%; 95% CI, 1.8–11.0%). The incidence rates of de novo HCC was significantly higher in the non-clean liver group than the clean liver group ($P = 0.003$, Fig. 3). In the remaining six patients, HCC developed at the same site of the initial nodules exclusively in 18 patients of a non-clean liver group by definition, and those HCC arose among the nodules of 8 mm or more in the initial MRI study.

Risk factors for HCC development

Univariate analyses showed that the significant risk factors for HCC development included older age ($P = 0.039$), cirrhosis ($P = 0.009$), a low platelet count ($P = 0.003$), a high AFP concentration ($P = 0.006$) and a non-clean liver ($P < 0.001$). Multivariate analysis with these variables revealed that older age (hazard ratio [HR], 1.08; 95% CI, 1.01–1.16; $P = 0.024$), a low plate-

Table 1 Baseline patient characteristics

Characteristics	Total ($n = 127$)	Non-clean liver ($n = 18$)	Clean liver ($n = 109$)	P
Age, years	65 (30–88)	68 (46–82)	64 (30–88)	0.15
Male/female	68/59	10/8	58/51	1.00
Non-cirrhosis/cirrhosis	59/68	6/12	53/56	0.31
HBV/HCV	26/101	5/13	21/88	0.53
Platelet count ($\times 10^9$/L)	122 (30–410)	102 (46–187)	125 (30–410)	0.07
ALT (IU/L)	32 (7–206)	32 (14–95)	32 (7–206)	0.97
γ-GT (IU/L)	31 (9–305)	31 (13–258)	31 (9–305)	0.68
AFP (ng/mL)	4 (1–582)	8 (2–181)	4 (1–582)	0.19

Continuous data are shown as medians (range).
γ-GT, γ-glutamyltransferase; AFP, α-fetoprotein; ALT, alanine aminotransferase; HBV, hepatitis B virus; HCV, hepatitis C virus.

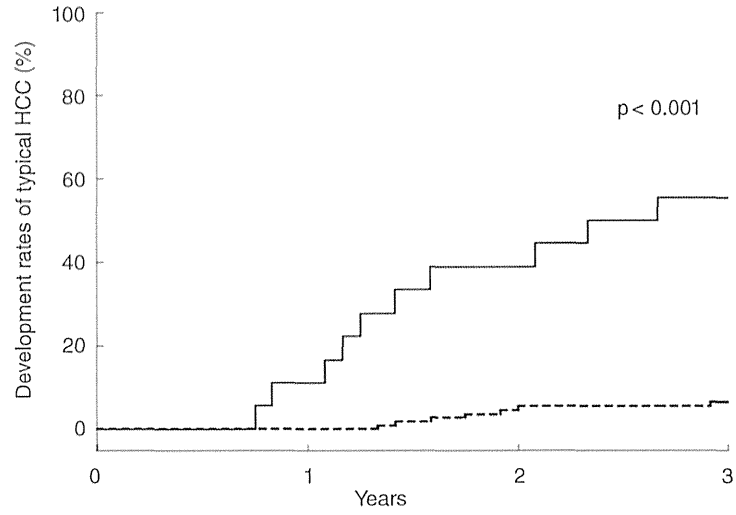

No. of patients at risk

Non-clean liver	18	16	11	8
Clean liver	109	109	103	102

Figure 2 Cumulative incidence rates of typical hepatocellular carcinoma (HCC) development in the non-clean and clean liver groups. —, non-clean liver group ($n = 18$); ----, clean liver group ($n = 109$).

let count (HR, 1.17; 95% CI, 1.03–1.35; $P = 0.017$) and a non-clean liver (HR, 9.41; 95% CI, 3.47–25.46; $P < 0.001$) were the only independent risk factors for HCC development (Table 2).

We further assessed the effect of a non-clean liver on the risk of HCC development in subgroups of these patients (Fig. 4). We found that belonging to the non-clean liver group was a significant risk factor in patients without HBV. Notably, this designation was particularly valuable for patients who are generally regarded as at low risk for HCC development: those without cirrhosis (HR, 37.23; 95% CI, 3.30–419.71; $P = 0.003$) and those with high platelet counts (HR, 33.42; 95% CI, 6.69–166.94; $P < 0.001$).

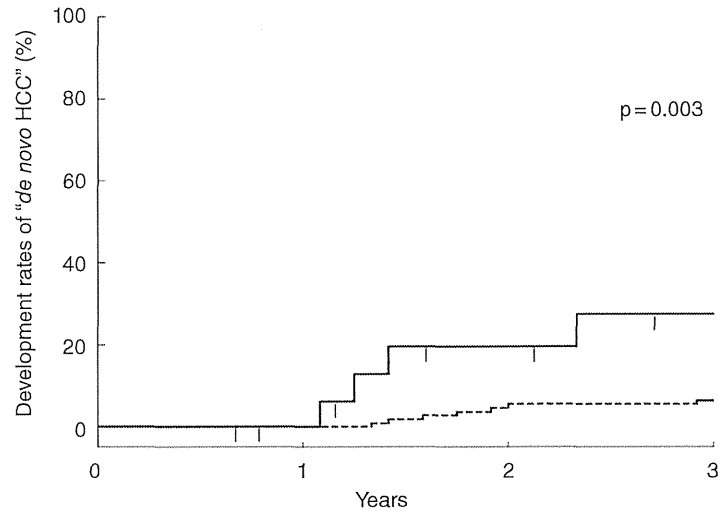

No. of patients at risk

Non-clean liver	18	18	15	14
Clean liver	109	109	103	102

Figure 3 Cumulative incidence rates of typical hepatocellular carcinoma (HCC) at sites in which no nodules had been seen on the initial gadoxetic acid-enhanced magnetic resonance imaging, namely, "de novo HCC". —, non-clean liver group ($n = 18$); ----, clean liver group ($n = 109$).

Table 2 Variables that predict HCC development: univariate and multivariate analyses

Variables	Univariate		Multivariate	
	Hazard ratio (95% CI)	*P*	Hazard ratio (95% CI)	*P*
Male	0.56 (0.29–1.95)	0.755		
Age (per year)	1.06 (1.00–1.12)	0.039	1.08 (1.01–1.16)	0.024
Cirrhosis	14.37 (1.90–108.44)	0.009	3.54 (0.37–33.77)	0.231
HCV (vs HBV)	4.39 (0.58–33.17)	0.151		
Platelet count (per 10^{10}/L)	1.19 (1.06–1.33)	0.003	1.17 (1.03–1.35)	0.017
ALT (per IU/L)	1.00 (0.99–1.02)	0.423		
γ-GT (per IU/L)	1.00 (0.99–1.01)	0.688		
AFP >10 ng/mL	3.98 (1.47–10.77)	0.006	1.47 (0.49–4.33)	0.486
Non-clean liver	12.36 (4.68–32.61)	<0.001	9.41 (3.47–25.46)	<0.001

γ-GT, γ-glutamyltransferase; AFP, α-fetoprotein; ALT, alanine aminotransferase; CI, confidence interval; HBV, hepatitis B virus; HCC, hepatocellular carcinoma; HCV, hepatitis C virus.

DISCUSSION

THIS STUDY REVEALED presence of hypovascular hypointense liver nodules (non-clean liver) on gadoxetic acid-enhanced MRI, is a significant risk factor for subsequent development of typical HCC not only at the same sites but also at the different sites from the initial nodules. The incidence of development of typical HCC in the non-clean liver patients was more than 50% during a 3-year follow-up period, indicating that these higher risk patients should be rigorously investigated for the early detection of HCC during follow up.

In the present study, six of the 18 patients in the non-clean liver group developed typical HCC at the same site of the initial nodules during the subsequent 3 years (11.1%/year). Most of the hypovascular hypointense nodules on gadoxetic acid-enhanced MRI are considered precursor lesions of typical HCC, such as early HCC or high-grade dysplastic nodules, on histological examination,[13–15] while it has been reported that most hypovascular nodules exhibiting high-intensity to isointensity signals in the hepatocyte phase are benign hepatic nodules.[14,15] Recent studies have suggested that a reduction of organic anion-transporting polypeptide 1B3 (OATP 8) transporter expression begins at the earliest stage of hepatocarcinogenesis,[21,22] before changes in vascularity such as decreased portal flow or increased arterial flow. The progression rate of the small

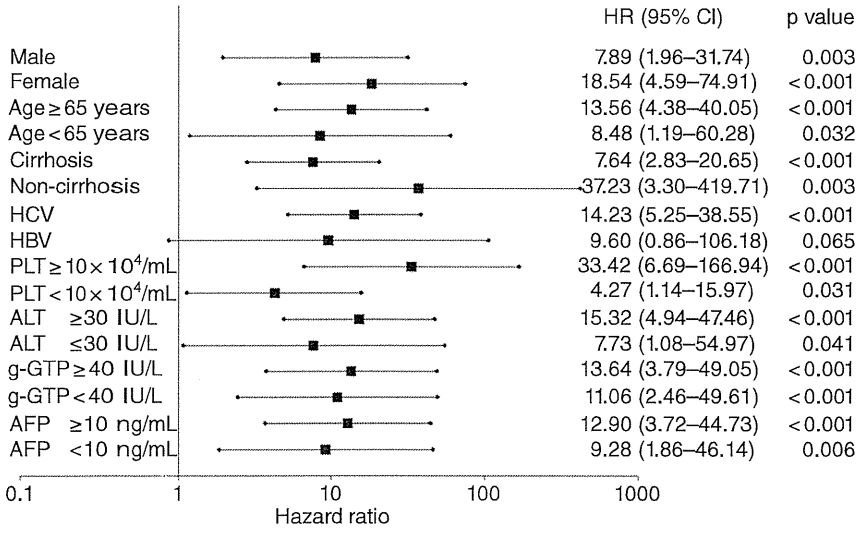

Figure 4 Stratified analyses of the non-clean liver as a risk factor for typical HCC development. AFP, α-fetoprotein; ALT, alanine aminotransferase; CI, confidence interval; g-GTP, γ-glutamyltransferase; HBV, hepatitis B virus; HCC, hepatocellular carcinoma; HCV, hepatitis C virus; HR, hazard ratio; PLT, platelets.

hypovascular hypointense nodules to typical HCC was reported as 10–17%/year,[9,10] which is comparable to the present study. Typical HCC arose exclusively among the nodules of 8 mm or more, as in previous studies in which the larger hypovascular hypointense nodules were found to be the risk factor for progression to typical HCC in the initial MRI study.[9,10]

Hyperintensity on T2WI[12] or diffusion-weighted images (DWI)[11] also was reported to be useful for prediction of typical HCC progress in hypovascular hypointense nodules. In our patients, none of the nodules in the non-clean liver group showed hyperintensity on T2WI, suggesting that the hepatocyte phase is more sensitive for detecting the early stage of hepatocarcinogenesis.[15] DWI were not evaluated in this study because this usually detects pathologically advanced HCC of larger size or with hypervascularity.[23] Thus, it is reasonable that the hepatocyte phase can effectively recognize the earliest stage of HCC development without T2WI or DWI.

In 11 of 17 patients, typical HCC developed at sites other than the initially detected hypovascular hypointense nodules. As shown in Figure 3, the incidence rates of such HCC in the non-clean liver group was significantly higher than in the clean liver group ($P = 0.003$), indicating that a non-clean liver itself is a risk factor for HCC development, apart from the detectable hypovascular hypointense nodules. In addition, in four patients with nodules even below 8 mm, two developed HCC at different sites from the initial nodules during follow up (data not shown). Taken together, a non-clean liver has the higher potential for hepatocarcinogenesis or for undetectable precursor lesions. The non-clean liver may reflect more advanced genetic or epigenetic changes in the background hepatocytes, however, the detailed biological mechanism is not clear in this study.

Non-clean liver was an independent risk factor for the development of typical HCC, apart from well-documented risk factors (Table 2), such as cirrhosis,[24] ALT,[25] γ-GT,[26] age and AFP.[27] A non-clean liver is a significant risk for HCC development also for those without cirrhosis or with high platelet counts (Fig. 4). This means patients at increased risk of HCC development can be discerned as having a non-clean liver even among low-risk subgroups.

Conversely, patients without such nodules (clean liver group) showed a significantly lower risk of developing typical HCC than those with non-clean livers (0.0% vs 11.1% at 1 year, 6.8% vs 55.5% at 3 years of follow up; $P < 0.001$), suggesting that gadoxetic acid-enhanced MRI could detect precursor lesions sensitively enough to rule out immediate (within 1 year) development of typical HCC. Although seven patients in the clean liver group developed typical HCC only after 1 year, these patients had other risk factors for HCC development, including lower platelet counts, implying more advanced liver cirrhosis or high AFP (data not shown). Such HCC may arise from precursor lesions that cannot be visualized by current imaging techniques.

This study is a retrospective study and has some limitations. We included patients with HBV and HCV together, because gadoxetic acid-enhanced MRI findings or HCC development do not differ between these two groups and HBV or HCV infection is not an independent risk factor for typical HCC development. However, the number of HBV patients was too small ($n = 26$) to statistically confirm the current result when limited to HBV patients only. Prospective studies with larger numbers of patients who have uniform liver disease etiologies and imaging intervals are needed to verify our findings in different settings. Although the imaging interval of the non-clean liver group was shorter than the clean liver group (3 vs 4 months: $P = 0.015$), the median intervals between the initial MRI and HCC diagnosis was 16 months in the non-clean liver group and 21 months in the clean liver group. They are short enough for cumulative detection of HCC development for 3 years and it is assumed that there was little influence on the conclusions.

In conclusion, patients with chronic viral liver disease are at high risk for developing typical HCC at any sites of the liver if they have hypovascular hypointense nodules on gadoxetic acid-enhanced MRI. These patients should be closely followed up for developing typical HCC not only at the same site but also at different sites from the initial nodule.

REFERENCES

1 Ichikawa T, Saito K, Yoshioka N *et al.* Detection and characterization of focal liver lesions: a Japanese phase III, multicenter comparison between gadoxetic acid disodium-enhanced magnetic resonance imaging and contrast-enhanced computed tomography predominantly in patients with hepatocellular carcinoma and chronic liver disease. *Invest Radiol* 2010; **45:** 133–41.
2 Halavaara J, Breuer J, Ayuso C *et al.* Liver tumor characterization: comparison between liver-specific gadoxetic acid disodium-enhanced MRI and biphasic CT – a multicenter trial. *J Comput Assist Tomogr* 2006; **30:** 345–54.
3 Hamm B, Staks T, Muhler A *et al.* Phase I clinical evaluation of Gd-EOB-DTPA as a hepatobiliary MR contrast

agent: safety, pharmacokinetics, and MR imaging. *Radiology* 1995; **195:** 785–92.
4 Hammerstingl R, Huppertz A, Breuer J *et al.* European EOB-study group. Diagnostic efficacy of gadoxetic acid (Primovist)-enhanced MRI and spiral CT for a therapeutic strategy: comparison with intraoperative and histopathologic findings in focal liver lesions. *Eur Radiol* 2008; **18:** 457–67.
5 Huppertz A, Balzer T, Blakeborough A *et al.* European EOB Study Group. Improved detection of focal liver lesions at MR imaging: multicenter comparison of gadoxetic acid-enhanced MR images with intraoperative findings. *Radiology* 2004; **230** (1): 266–75.
6 Di Martino M, Marin D, Guerrisi A *et al.* Intraindividual comparison of gadoxetate disodium-enhanced MR imaging and 64-section multidetector CT in the detection of hepatocellular carcinoma in patients with cirrhosis. *Radiology* 2010; **256:** 806–16.
7 Inoue T, Kudo M, Komuta M *et al.* Assessment of Gd-EOB-DTPA-enhanced MRI for HCC and dysplastic nodules and comparison of detection sensitivity versus MDCT. *J Gastroenterol* 2012; **47:** 1036–47.
8 Golfieri R, Renzulli M, Lucidi V, Corcioni B, Trevisani F, Bolondi L. Contribution of the hepatobiliary phase of Gd-EOB-DTPA-enhanced MRI to dynamic MRI in the detection of hypovascular small (</= 2 cm) HCC in cirrhosis. *Eur Radiol* 2011; **21:** 1233–42.
9 Kumada T, Toyoda H, Tada T *et al.* Evolution of hypointense hepatocellular nodules observed only in the hepatobiliary phase of gadoxetate disodium-enhanced MRI. *AJR Am J Roentgenol* 2011; **197** (1): 58–63.
10 Motosugi U, Ichikawa T, Sano K *et al.* Outcome of hypovascular hepatic nodules revealing no gadoxetic acid uptake in patients with chronic liver disease. *J Magn Reson Imaging* 2011; **34** (1): 88–94.
11 Kim YK, Lee WJ, Park MJ, Kim SH, Rhim H, Choi D. Hypovascular hypointense nodules on hepatobiliary phase gadoxetic acid-enhanced MR images in patients with cirrhosis: potential of DW imaging in predicting progression to hypervascular HCC. *Radiology* 2012; **265** (1): 104–14.
12 Hyodo T, Murakami T, Imai Y *et al.* Hypovascular nodules in patients with chronic liver disease: risk factors for development of hypervascular hepatocellular carcinoma. *Radiology* 2013; **266:** 480–90.
13 Bartolozzi C, Battaglia V, Bargellini I *et al.* Contrast-enhanced magnetic resonance imaging of 102 nodules in cirrhosis: correlation with histological findings on explanted livers. *Abdom Imaging* 2013; **38:** 290–6.
14 Golfieri R, Grazioli L, Orlando E *et al.* Which is the best MRI marker of malignancy for atypical cirrhotic nodules: hypointensity in hepatobiliary phase alone or combined with other features? Classification after Gd-EOB-DTPA administration. *J Magn Reson Imaging* 2012; **36:** 648–57.
15 Sano K, Ichikawa T, Motosugi U *et al.* Imaging study of early hepatocellular carcinoma: usefulness of gadoxetic acid-enhanced MR imaging. *Radiology* 2011; **261:** 834–44.
16 Motosugi U. Hypovascular hypointense nodules on hepatocyte phase gadoxetic acid-enhanced MR images: too early or too progressed to determine hypervascularity. *Radiology* 2013; **267** (1): 317–8.
17 Asayama Y, Yoshimitsu K, Nishihara Y *et al.* Arterial blood supply of hepatocellular carcinoma and histologic grading: radiologic-pathologic correlation. *AJR Am J Roentgenol* 2008; **190** (1): W28–34.
18 Motosugi U, Ichikawa T, Sou H *et al.* Liver parenchymal enhancement of hepatocyte-phase images in Gd-EOB-DTPA-enhanced MR imaging: which biological markers of the liver function affect the enhancement? *J Magn Reson Imaging* 2009; **30:** 1042–6.
19 Bruix J, Sherman M, American Association for the Study of Liver Diseases. Management of hepatocellular carcinoma: an update. *Hepatology* 2011; **53:** 1020–2.
20 Motosugi U, Ichikawa T, Araki T. Rules, roles, and room for discussion in gadoxetic acid-enhanced magnetic resonance liver imaging: current knowledge and future challenges. *Magnetic Rsonance in Medical Sciences.* 2013; **12:** 161–75.
21 Kitao A, Zen Y, Matsui O *et al.* Hepatocellular carcinoma: signal intensity at gadoxetic acid-enhanced MR imaging – correlation with molecular transporters and histopathologic features. *Radiology* 2010; **256:** 817–26.
22 Narita M, Hatano E, Arizono S *et al.* Expression of OATP1B3 determines uptake of Gd-EOB-DTPA in hepatocellular carcinoma. *J Gastroenterol* 2009; **44:** 793–8.
23 Nasu K, Kuroki Y, Tsukamoto T, Nakajima H, Mori K, Minami M. Diffusion-weighted imaging of surgically resected hepatocellular carcinoma: imaging characteristics and relationship among signal intensity, apparent diffusion coefficient, and histopathologic grade. *American Journal of Roentgenology* 2009; **193:** 438–44.
24 Degos F, Christidis C, Ganne-Carrie N *et al.* Hepatitis C virus related cirrhosis: time to occurrence of hepatocellular carcinoma and death. *Gut* 2000; **47** (1): 131–6.
25 Tarao K, Rino Y, Ohkawa S *et al.* Association between high serum alanine aminotransferase levels and more rapid development and higher rates of incidence of hepatocellular carcinoma in patients with hepatitis C virus-associated cirrhosis. *Cancer* 1999; **86:** 589–95.
26 Ikeda K, Saitoh S, Suzuki Y *et al.* Disease progression and hepatocellular carcinogenesis in patients with chronic viral hepatitis: a prospective observation of 2215 patients. *J Hepatol* 1998; **28:** 930–8.
27 Ikeda K, Saitoh S, Koida I *et al.* A multivariate analysis of risk factors for hepatocellular carcinogenesis: a prospective observation of 795 patients with viral and alcoholic cirrhosis. *Hepatology* 1993; **18** (1): 47–53.

Hepatology Research

Hepatology Research 2014; 44: 720–727 doi: 10.1111/hepr.12179

Original Article

Prospective comparison of real-time tissue elastography and serum fibrosis markers for the estimation of liver fibrosis in chronic hepatitis C patients

Nobuharu Tamaki,[1] Masayuki Kurosaki,[1] Shuya Matsuda,[1] Toru Nakata,[1] Masaru Muraoka,[1] Yuichiro Suzuki,[1] Yutaka Yasui,[1] Shoko Suzuki,[1] Takanori Hosokawa,[1] Takashi Nishimura,[1] Ken Ueda,[1] Kaoru Tsuchiya,[1] Hiroyuki Nakanishi,[1] Jun Itakura,[1] Yuka Takahashi,[1] Kotaro Matsunaga,[2,4] Kazuhiro Taki,[2] Yasuhiro Asahina[3] and Namiki Izumi[1]

Divisions of [1]Gastroenterology and Hepatology and [2]Pathology, Musashino Red Cross Hospital, [3]Division of Gastroenterology and Hepatology, Tokyo Medical and Dental University, Tokyo and [4]Division of Gastroenterology and Hepatology, St Marianna University School of Medicine, Kanagawa, Japan

Aim: Real-time tissue elastography (RTE) is a non-invasive method for the measurement of tissue elasticity using ultrasonography. Liver fibrosis (LF) index is a quantitative method for evaluation of liver fibrosis calculated by RTE image features. This study aimed to investigate the significance of LF index for predicting liver fibrosis in chronic hepatitis C patients.

Methods: In this prospective study, 115 patients with chronic hepatitis C who underwent liver biopsy were included, and the diagnostic accuracy of LF index and serum fibrosis markers was evaluated.

Results: RTE imaging was successfully performed on all patients. Median LF index in patients with F0–1, F2, F3 and F4 were 2.61, 3.07, 3.54 and 4.25, respectively, demonstrating a stepwise increase with liver fibrosis progression ($P < 0.001$). LF index (odds ratio [OR] = 5.3, 95% confidence interval [CI] = 2.2–13.0) and platelet count (OR = 0.78, 95% CI = 0.68–0.89) were independently associated with the presence of advanced fibrosis (F3–4). Further, LF index was independently associated with the presence of minimal fibrosis (F0–1) (OR = 0.25, 95% CI = 0.11–0.55). The area under the receiver–operator curve (AUROC) of LF index for predicting advanced fibrosis (0.84) was superior to platelets (0.82), FIB-4 index (0.80) and aspartate aminotransferase/platelet ratio index (APRI) (0.76). AUROC of LF index (0.81) was superior to platelets (0.73), FIB-4 index (0.79) and APRI (0.78) in predicting minimal fibrosis.

Conclusion: LF index calculated by RTE is useful for predicting liver fibrosis, and diagnostic accuracy of LF index is superior to serum fibrosis markers.

Key words: chronic hepatitis C, fibrosis, liver fibrosis index, real-time tissue elastography

INTRODUCTION

AN ADVANCED STAGE of liver fibrosis in chronic hepatitis C (CHC) is associated with hepatocellular carcinoma development and complications such as esophageal variceal bleeding and liver failure.[1,2] Therefore, accurate evaluation of the stage of liver fibrosis is most important in clinical practice. Liver biopsy is considered to be the golden standard for diagnosis of liver fibrosis.[3–5] However, this method may be inaccurate because of sampling errors and interobserver variations.[6,7]

Improvements in a variety of non-invasive methods for evaluating liver fibrosis have recently emerged as alternatives to liver biopsy. Liver fibrosis was reportedly predicted by measurement of liver stiffness using transient elastography[8,9] and acoustic radiation force impulse (ARFI).[10,11] As assessed by blood laboratory tests, the aspartate aminotransferase (AST)/alanine

Correspondence: Dr Namiki Izumi, Department of Gastroenterology and Hepatology, Musashino Red Cross Hospital, 1-26-1 Kyonan-cho, Musashino-shi, Tokyo 180-8610, Japan. Email: nizumi@musashino.jrc.or.jp

Conflict of interest: The authors who have taken part in this study declare that they do not have anything to disclose regarding funding or conflict of interest with respect to this manuscript.

Received 28 January 2013; revision 20 May 2013; accepted 29 May 2013.

aminotransferase (ALT) ratio,[12] AST/platelet ratio index (APRI),[13,14] and FIB-4 index[15,16] have been reported to be useful for the prediction of liver fibrosis. We previously reported that the FIB-4 index is useful for the prediction of liver fibrosis progression.[17]

Real-time tissue elastography (RTE) is a non-invasive method for the measurement of tissue elasticity using ultrasonography.[18] RTE calculates the relative hardness of tissue from the degree of tissue distortion and displays this information as a color image. RTE was recently reported to be useful for predicting liver fibrosis.[19,20] To increase the objectivity of the evaluation, an image analysis method to evaluate the strain image features and a new algorithm to deliver an index were proposed. Liver fibrosis (LF) index is a quantitative method for evaluation of liver fibrosis that is calculated by nine RTE image features, and the significance of LF index for predicting liver fibrosis has been reported.[21,22]

In the present study, we prospectively investigated the significance of LF index calculated by RTE for the prediction of liver fibrosis in CHC patients. Further, diagnostic accuracy for liver fibrosis was compared between LF index and serum fibrosis markers.

METHODS

Patients

A TOTAL OF 127 consecutive patients with CHC were prospectively investigated. All patients underwent liver biopsy at Musashino Red Cross Hospital between February 2011 and November 2012. Exclusion criteria comprised the following: (i) co-infection with hepatitis B virus ($n = 1$); (ii) co-infection with HIV ($n = 1$); (iii) history of autoimmune hepatitis or primary biliary cirrhosis ($n = 3$); (iv) alcohol abuse (intake of alcohol equivalent to pure alcohol ≥40 g/day) ($n = 0$); (v) portal tracts of biopsy sample of less than five ($n = 7$); and (vi) presence of serious heart disease ($n = 0$). After exclusion, 115 patients were enrolled in this study. Written informed consent was obtained from each patient and the study protocol conformed to the ethical guidelines of the Declaration of Helsinki and was approved by the institutional ethics review committees (application no. 24007).

Histological evaluation

Liver biopsy specimens were laparoscopically obtained using 13-G needles ($n = 93$). When laparoscopy was not conducted due to a history of upper abdominal surgery, percutaneous ultrasound-guided liver biopsy was performed using 15-G needles ($n = 22$). Specimens were fixed, paraffin-embedded, and stained with hematoxylin–eosin and Masson-trichrome. A biopsy sample with minimum portal tracts of five was required for diagnosis. All liver biopsy samples were independently evaluated by two senior pathologists who were blinded to the clinical data. Fibrosis staging was categorized according to the METAVIR score:[23] F0, no fibrosis; F1, portal fibrosis without septa; F2, portal fibrosis with few septa; F3, numerous septa without cirrhosis; and F4, cirrhosis. Activity of necroinflammation was graded on a scale of 0–3: A0, no activity; A1, mild activity; A2, moderate activity; and A3, severe activity. Percentage of steatosis was quantified by determining the average proportion of hepatocytes affected by steatosis and graded on a scale of 0–3: grade 0, no steatosis; grade 1, 1–33%; grade 2, 34–66%; and grade 3, 67% and over.

Clinical and biological data

The age and sex of the patients were recorded. Serum samples were collected within 1 day prior to liver biopsy and the following variables were obtained through serum sample analysis: AST, ALT and platelet count. FIB-4 index and APRI were calculated according to the published formula appropriate to each measure.[13,15]

RTE and LF index

Real-time tissue elastography was performed using HI VISION Preirus (Hitachi Aloka Medical, Tokyo, Japan) and the EUP-L52 linear probe (3–7 MHz; Hitachi Aloka Medical) within 3 days of liver biopsy. RTE was performed on the right lobe of the liver through the intercostal space. An RTE image was induced by heartbeats. Five RTE images were collected for each patient and analyzed to calculate nine image features. RTE method and the equation that calculates LF index using nine image features has been previously detailed.[22] Results are expressed as mean LF index of all measurements. Two hepatologists (N. T. and K. Tsuchiya, with 8 and 16 years of experience, respectively) performed RTE. In 32 patients with CHC, LF index was measured independently by two examiners. The correlation coefficient of LF index between two examiners was 0.85 ($P \leq 0.001$).

Statistical analysis

Correlations between LF index and histological fibrosis stage were analyzed using Spearman's rank correlation coefficients. Categorical variables were compared using Fisher's exact test, and continuous variables were compared using Mann–Whitney *U*-test. $P < 0.05$ was considered statistically significant. Logistic regression was

used for multivariate analysis. Receiver–operator curves (ROC) were constructed, and the area under the ROC (AUROC) was calculated. Optimal cut-off values were selected, to maximize sensitivity, specificity and diagnostic accuracy. Sensitivity, specificity, positive predictive value (PPV) and negative predictive value (NPV) were calculated by using cut-offs obtained by ROC. SPSS software ver. 15.0 (SPSS, Chicago, IL, USA) was used for analyses.

RESULTS

Patient characteristics

THE CHARACTERISTICS OF all 115 patients are listed in Table 1. F0–1 was diagnosed in 52 cases (45%), F2 in 31 (27%), F3 in 20 (17%) and F4 in 12 (11%). Mean values of LF index of F0 (2.62) and F1 (2.60) were not significantly different ($P = 0.9$), and only six patients with F0 were included in this study. Therefore, patients with F0 and F1 were integrated for the analysis. RTE imaging was successfully performed in all patients, and LF index was calculated.

Relationship between histological findings and LF index by RTE

The median value of LF index compared with the METAVIR fibrosis stage is shown in Figure 1. Median LF index in patients with F0–1, F2, F3 and F4 were 2.61, 3.07, 3.54 and 4.25, respectively, demonstrating a stepwise increase with liver fibrosis progression ($P < 0.001$). LF index of each fibrosis stage significantly differed from each other (F0–1 vs F2, $P < 0.001$; F0–1 vs F3, $P < 0.001$; F0–1 vs F4, $P < 0.001$; F2 vs F3, $P = 0.009$; F2 vs F4, $P = 0.001$). On the other hand, mean values of LF index in patients with steatosis grade 0, 1 and 2 were 2.99, 3.29 and 2.60, respectively, demonstrating no significant correlation (Fig. 2a). LF index was compared with steatosis grade for each fibrosis stage. LF index was not significantly different between patients with steatosis and without steatosis (Fig. 2b).

Liver fibrosis index was compared with histological activity. A significant correlation existed between histological activity and fibrosis stage. Therefore, the relationship between LF index and histological activity was examined by each fibrosis stage. In patients with F0–1, the mean LF index of A1, A2 and A3 was 2.60, 2.58 and 2.40, respectively, demonstrating no significant correlation. Similarly, in patients with F2, F3 and F4, there was no significant correlation between LF index and histological activity (Fig. 3).

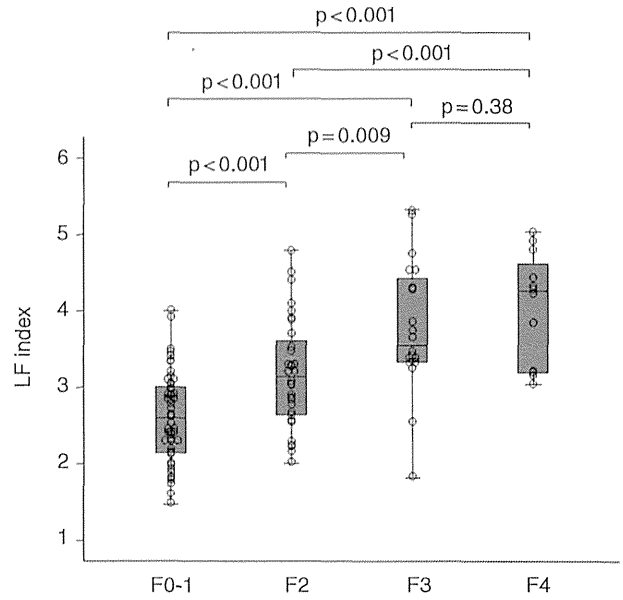

Figure 1 Correlation between liver fibrosis (LF) index calculated by real-time tissue elastography and fibrosis stage. Box plot of the LF index is shown according to each fibrosis stage. The bottom and top of each box represent the 25th and 75th percentiles, giving the interquartile range. The line through the box indicates the median value, and error bar indicates minimum and maximum non-extreme values.

Table 1 Patient characteristics

Characteristics	Patients ($n = 115$)
Female/male	68/47
Age (years)	57.9 ± 10.9
AST (IU/L)	55.7 ± 44.9
ALT (IU/L)	63.2 ± 56.3
Platelet counts ($\times 10^9$/L)	162 ± 53
Portal tracts of biopsy samples	12.6 ± 5.0
Fibrosis stage	
F0–1 (%)	51 (44)
F2 (%)	32 (28)
F3 (%)	20 (17)
F4 (%)	12 (11)
Histological activity	
A0 (%)	0 (0)
A1 (%)	75 (65)
A2 (%)	34 (30)
A3 (%)	6 (5)
Steatosis grade	
Grade 0 (%)	65 (57)
Grade 1 (%)	47 (41)
Grade 2 (%)	3 (2)
Grade 3 (%)	0 (0)

ALT, alanine aminotransferase; AST, aspartate aminotransferase.

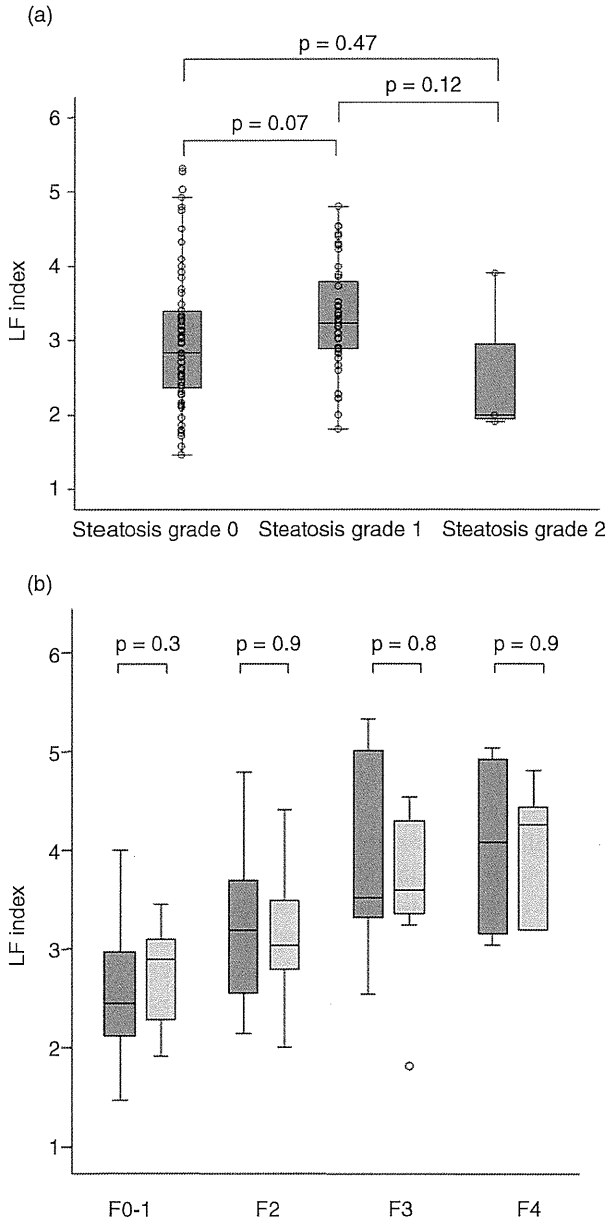

Figure 2 (a) Correlation between liver fibrosis (LF) index and steatosis grade. Box plot of the LF index is shown according to each steatosis grade. The bottom and top of each box represent the 25th and 75th percentiles, giving the interquartile range. The line through the box indicates the median value, and error bar indicates minimum and maximum non-extreme values. (b) Box plot of LF index for each fibrosis stage in relation to degree of steatosis grade. The bottom and top of each box represent the 25th and 75th percentiles, giving the interquartile range. The line through the box indicates the median value, and error bar indicates minimum and maximum non-extreme values. Dark grey bar chart indicates steatosis grade 0. Light grey bar chart indicates steatosis grade 1–2.

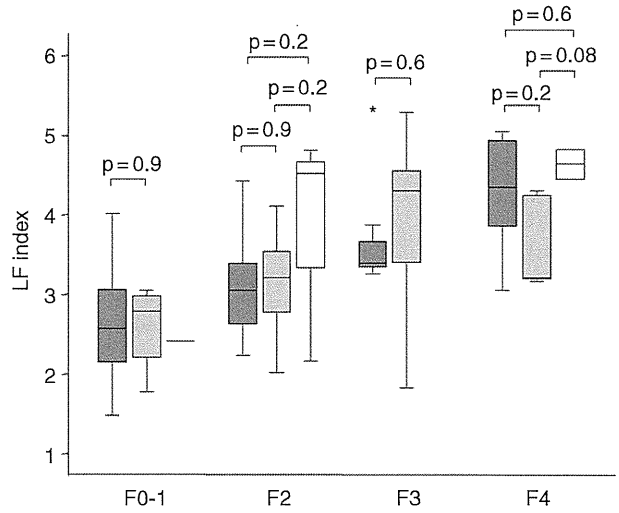

Figure 3 Box plot of liver fibrosis (LF) index for each fibrosis stage in relation to degree of necroinflammatory activity. The bottom and top of each box represent the 25th and 75th percentiles, giving the interquartile range. The line through the box indicates the median value, and error bar indicates minimum and maximum non-extreme values. Dark grey bar chart indicates activity grade 1. Light grey bar chart indicates activity grade 2. White bar chart indicates activity grade 3.

Comparison of variables associated with the presence of advanced fibrosis (F3–4) by univariate and multivariate analysis

Variables associated with the presence of advanced fibrosis (F3–4) were assessed by univariate and multivariate analysis (Table 2). The variables of age ($P = 0.03$) and LF index ($P < 0.001$) were significantly higher, and the variable of platelets ($P < 0.001$) was significantly lower in patients with advanced fibrosis than in patients with F0–2. Multivariate analysis showed that LF index (odds ratio [OR] = 5.3, 95% confidence interval [CI] =2.2–13.0) and platelets (OR = 0.78, 95% CI = 0.68–0.89) were independently associated with the presence of advanced fibrosis.

Comparison of variables associated with the presence of minimal fibrosis (F0–1) by univariate and multivariate analysis

Variables associated with the presence of minimal fibrosis (F0–1) were assessed by univariate and multivariate analysis (Table 3). The variables of age ($P < 0.001$), AST ($P = 0.02$) and LF index ($P < 0.001$) were significantly lower, and the variable of platelets ($P < 0.001$) was significantly higher in F0–1 patients than F2–4 patients.

Table 2 Variables associated with the presence of advanced fibrosis (F3–4) by univariate and multivariate analysis

	F0–2 ($n = 83$)	F3–4 ($n = 32$)	*P*-value (Univariate)	Odds ratio (95% CI) (Multivariate)
Age (years)	56.6 ± 10.9	61.3 ± 10.4	0.03	
Sex (female/male)	51/32	17/15	0.41	
AST (IU/L)	52.3 ± 43.3	64.4 ± 48.3	0.19	
ALT (IU/L)	62.9 ± 60.6	63.9 ± 44.2	0.93	
Platelets ($\times 10^9$/L)	179 ± 47	117 ± 42	<0.001	0.78 (0.68–0.89)
LF index	2.81 ± 0.69	3.86 ± 0.81	<0.001	5.30 (2.16–13.0)

ALT, alanine aminotransferase; AST, aspartate aminotransferase; CI, confidence interval; LF, liver fibrosis.

Multivariate analysis showed that LF index was independently associated with the presence of minimal fibrosis (OR = 0.25, 95% CI = 0.11–0.55).

Diagnostic accuracy of RTE and serum fibrosis markers

Receiver-operator curves of LF index, platelets, FIB-4 index and APRI for predicting advanced fibrosis (F3–4), and minimal fibrosis (F0–1) were plotted, as shown in Figure 4. AUROC of LF index for predicting advanced fibrosis (0.84) was superior to platelets (0.82), FIB-4 index (0.80) and APRI (0.76). Similarly, for predicting minimal fibrosis, AUROC of LF index (0.81) was superior to platelets (0.73), FIB-4 index (0.79) and APRI (0.78). The corresponding sensitivities, specificities, PPV and NPV are detailed in Table 4.

DISCUSSION

IMPROVEMENTS IN VARIOUS methods for prediction of liver fibrosis have recently emerged as alternatives to liver biopsy. RTE is a non-invasive method for the measurement of tissue elasticity using ultrasonography. The utility of RTE for evaluating liver fibrosis is reported in a few studies.[18–22] However, for utilizing LF index, one of the equations used to calculate tissue elasticity by RTE is still unclear. The aim of this study was to investigate the significance of LF index for the prediction of liver fibrosis in CHC patients.

In this prospective study, we found that LF index is a useful predictive factor for diagnosis of the fibrosis stage in CHC patients. Increase in LF index significantly correlated with progression of the fibrosis stage and LF index was able to predict the presence of advanced fibrosis and minimal fibrosis. Previous studies reported the utility of LF index for prediction of the liver fibrosis stage.[21,22] In this study, LF index differed significantly between patients with F0–1 and F2; thus, LF index was especially useful for prediction of minimal fibrosis. This may be due to a sufficient number of patients with F0–1 and F2 included in the present study. This is an advantage of LF index because other quantitative methods by RTE could not discriminate patients with F0–1 and F2.[19,20] On the other hand, there is a possibility that a similar result may be obtained for differentiation of F3 and F4 if a large number of patients with advanced fibrosis was included.

Previous studies did not compare the diagnostic accuracy of LF index and serum fibrosis markers. We revealed that LF index performed better than serum fibrosis

Table 3 Variables associated with the presence of minimal fibrosis (F0–1) by univariate and multivariate analysis

	F0–1 ($n = 51$)	F2–4 ($n = 64$)	*P*-value (Univariate)	Odds ratio (95% CI) (Multivariate)
Age (years)	54.0 ± 11.9	61.0 ± 9.0	<0.001	
Sex (female/male)	31/20	37/27	0.74	
AST (IU/L)	44.5 ± 42.6	64.6 ± 44.9	0.02	
ALT (IU/L)	53.0 ± 56.3	71.3 ± 55.5	0.08	
Platelets ($\times 10^9$/L)	186 ± 47	142 ± 50	<0.001	
LF index	2.60 ± 0.59	3.51 ± 0.84	<0.001	0.25 (0.11–0.55)

ALT, alanine aminotransferase; AST, aspartate aminotransferase; CI, confidence interval; LF, liver fibrosis.

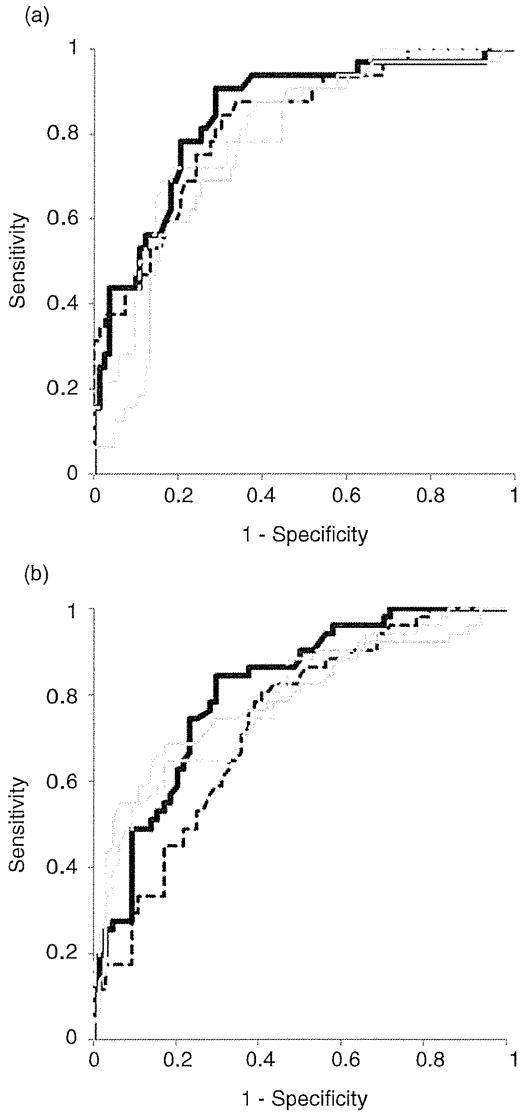

Figure 4 Receiver–operator curves (ROC) of liver fibrosis (LF) index and serum fibrosis markers. (a) ROC for diagnosis of significant fibrosis (F3–4). (b) ROC for diagnosis of minimal fibrosis (F0–1). —, LF index; ····, platelets; , aspartate aminotransferase-to-platelet ratio index; , FIB-4 index.

markers based on blood laboratory tests for predicting liver fibrosis.

Transient elastography has been most commonly used to measure liver stiffness and is established in clinical practice to evaluate liver fibrosis.[8,9] RTE exhibits some advantages compared with transient elastography. In this study, RTE imaging was successfully performed in all patients, and LF index was calculated. Although transient elastography has high diagnostic capabilities when it comes to liver fibrosis, measurements are sometimes impossible in patients with severe obesity and ascites.[24] Reproducibility of transient elastography was reportedly lower in patients with steatosis, inflammation, increased body mass index and lower degrees of liver fibrosis.[25–27] On the other hand, LF index is measured by ultrasound guidance that facilitates the identification of a suitable location for elastographic measurement, thereby resulting in a higher number of patients with valid results.

Unlike transient elastography, another advantage of LF index is that the results are not influenced by the presence of inflammation and steatosis. It was reported that LF index is not useful in patients with steatosis.[22] However, LF index was not significantly different between patients with and without steatosis in the present study even after stratification by fibrosis stage. Thus, LF index was useful for prediction of fibrosis in CHC patients regardless of steatosis. Because LF index of each activity grade and steatosis grade did not differ from each other, estimation of liver fibrosis by LF index demonstrated higher reproducibility than transient elastography.

In previously reports, diagnostic accuracy of liver fibrosis using RTE was inferior to transient elastography;[28] however, other studies have reported contrasting results.[19] The reason for this variability is probably because RTE technology and the equations used to calculate tissue elasticity are rapidly changing. The utility of elastic ratio, another RTE method for evaluation of liver fibrosis, was reported.[20] The elastic ratio is the ratio between the tissue compressibility of the liver and that of the intrahepatic small vessel. The AUROC of elastic ratio for predicting advanced fibrosis was 0.94 and was superior to LF index. Further, ARFI and real-time shear wave elastography were reported to have a high diagnostic accuracy of liver fibrosis.[10,11,29] There are currently no studies that directly compare LF index and those methods for diagnostic value of liver fibrosis. Therefore, further studies are needed to fully explore the potential of RTE, especially with regard to LF index.

Our study had several limitations. The number of patients with advanced fibrosis was small. The potential of LF index to differentiate patients with F3 and F4 needs to be explored with a large number of patients. Further, validation study is needed to evaluate the diagnostic accuracy of fibrosis stage, especially in comparison with other modalities.

In conclusion, LF index calculated by RTE is useful for predicting liver fibrosis, and diagnostic accuracy of LF index is superior to that of serum fibrosis markers.

Table 4 Diagnostic performance of LF index and serum fibrosis markers

	F0–2 vs F3–4					F0–1 vs F2–4				
	AUROC	Sensitivity (%)	Specificity (%)	PPV (%)	NPV (%)	AUROC	Sensitivity (%)	Specificity (%)	PPV (%)	NPV (%)
LF index	0.84	90.6	71.1	54.7	95.2	0.81	84.3	70.3	69.4	84.9
Platelets	0.82	87.5	66.3	50.0	93.2	0.73	80.4	59.4	61.2	79.2
FIB-4 index	0.80	71.9	81.9	60.5	88.3	0.79	54.9	90.6	82.3	71.6
APRI	0.76	87.5	61.4	46.7	92.7	0.78	64.7	85.9	78.6	75.3

APRI, aspartate aminotransferase/platelet ratio index; AUROC, area under the receiver-operator curve; NPV, negative predictive value; PPV, positive predictive value.

ACKNOWLEDGMENT

THIS STUDY WAS supported by a Grant-in-Aid from Ministry of Health, Labor, and Welfare, Japan.

REFERENCES

1 Serfaty L, Aumaitre H, Chazouilleres O *et al.* Determinants of outcome of compensated hepatitis C virus-related cirrhosis. *Hepatology* 1998; **27**: 1435–40.
2 Benvegnu L, Gios M, Boccato S, Alberti A. Natural history of compensated viral cirrhosis: a prospective study on the incidence and hierarchy of major complications. *Gut* 2004; **53**: 744–9.
3 Dienstag JL. The role of liver biopsy in chronic hepatitis C. *Hepatology* 2002; **36**: S152–60.
4 Gebo KA, Herlong HF, Torbenson MS *et al.* Role of liver biopsy in management of chronic hepatitis C: a systematic review. *Hepatology* 2002; **36**: S161–72.
5 Namiki I, Nishiguchi S, Hino K *et al.* Management of hepatitis C; Report of the Consensus Meeting at the 45th Annual Meeting of the Japan Society of Hepatology (2009). *Hepatol Res* 2010; **40**: 347–68.
6 Bedossa P, Dargere D, Paradis V. Sampling variability of liver fibrosis in chronic hepatitis C. *Hepatology* 2003; **38**: 1449–57.
7 Intraobserver and interobserver variations in liver biopsy interpretation in patients with chronic hepatitis C. The French METAVIR Cooperative Study Group. *Hepatology* 1994; **20**: 15–20.
8 Sandrin L, Fourquet B, Hasquenoph JM *et al.* Transient elastography: a new noninvasive method for assessment of hepatic fibrosis. *Ultrasound Med Biol* 2003; **29**: 1705–13.
9 Friedrich-Rust M, Ong MF, Martens S *et al.* Performance of transient elastography for the staging of liver fibrosis: a meta-analysis. *Gastroenterology* 2008; **134**: 960–74.
10 Friedrich-Rust M, Wunder K, Kriener S *et al.* Liver fibrosis in viral hepatitis: noninvasive assessment with acoustic radiation force impulse imaging versus transient elastography. *Radiology* 2009; **252**: 595–604.
11 Palmeri ML, Wang MH, Rouze NC *et al.* Noninvasive evaluation of hepatic fibrosis using acoustic radiation force-based shear stiffness in patients with nonalcoholic fatty liver disease. *J Hepatol* 2011; **55**: 666–72.
12 Williams AL, Hoofnagle JH. Ratio of serum aspartate to alanine aminotransferase in chronic hepatitis. Relationship to cirrhosis. *Gastroenterology* 1988; **95**: 734–9.
13 Wai CT, Greenson JK, Fontana RJ *et al.* A simple noninvasive index can predict both significant fibrosis and cirrhosis in patients with chronic hepatitis C. *Hepatology* 2003; **38**: 518–26.
14 Lin ZH, Xin YN, Dong QJ *et al.* Performance of the aspartate aminotransferase-to-platelet ratio index for the staging of hepatitis C-related fibrosis: an updated meta-analysis. *Hepatology* 2011; **53**: 726–36.
15 Sterling RK, Lissen E, Clumeck N *et al.* Development of a simple noninvasive index to predict significant fibrosis in patients with HIV/HCV coinfection. *Hepatology* 2006; **43**: 1317–25.
16 Vallet-Pichard A, Mallet V, Nalpas B *et al.* FIB-4: an inexpensive and accurate marker of fibrosis in HCV infection. comparison with liver biopsy and fibrotest. *Hepatology* 2007; **46**: 32–6.
17 Tamaki N, Kurosaki M, Tanaka K *et al.* Noninvasive estimation of fibrosis progression overtime using the FIB-4 index in chronic hepatitis C. *J Viral Hepat* 2013; **20**: 72–6.
18 Friedrich-Rust M, Ong MF, Herrmann E *et al.* Real-time elastography for noninvasive assessment of liver fibrosis in chronic viral hepatitis. *AJR Am J Roentgenol* 2007; **188**: 758–64.
19 Morikawa H, Fukuda K, Kobayashi S *et al.* Real-time tissue elastography as a tool for the noninvasive assessment of liver stiffness in patients with chronic hepatitis C. *J Gastroenterol* 2011; **46**: 350–8.
20 Koizumi Y, Hirooka M, Kisaka Y *et al.* Liver fibrosis in patients with chronic hepatitis C: noninvasive diagnosis by means of real-time tissue elastography – establishment of the method for measurement. *Radiology* 2011; **258**: 610–17.

21 Tatsumi C, Kudo M, Ueshima K *et al.* Non-invasive evaluation of hepatic fibrosis for type C chronic hepatitis. *Intervirology* 2010; **53:** 76–81.
22 Tomeno W, Yoneda M, Imajo K *et al.* Evaluation of the Liver Fibrosis Index calculated by using real-time tissue elastography for the non-invasive assessment of liver fibrosis in chronic liver diseases. *Hepatol Res* 2012; **12:** 12023.
23 Bedossa P, Poynard T. An algorithm for the grading of activity in chronic hepatitis C. The METAVIR Cooperative Study Group. *Hepatology* 1996; **24:** 289–93.
24 Castera L, Foucher J, Bernard PH *et al.* Pitfalls of liver stiffness measurement: a 5-year prospective study of 13,369 examinations. *Hepatology* 2010; **51:** 828–35.
25 Fraquelli M, Rigamonti C, Casazza G *et al.* Reproducibility of transient elastography in the evaluation of liver fibrosis in patients with chronic liver disease. *Gut* 2007; **56:** 968–73.
26 Arena U, Vizzutti F, Abraldes JG *et al.* Reliability of transient elastography for the diagnosis of advanced fibrosis in chronic hepatitis C. *Gut* 2008; **57:** 1288–93.
27 Rizzo L, Calvaruso V, Cacopardo B *et al.* Comparison of transient elastography and acoustic radiation force impulse for non-invasive staging of liver fibrosis in patients with chronic hepatitis C. *Am J Gastroenterol* 2011; **106:** 2112–20.
28 Colombo S, Buonocore M, Del Poggio A *et al.* Head-to-head comparison of transient elastography (TE), real-time tissue elastography (RTE), and acoustic radiation force impulse (ARFI) imaging in the diagnosis of liver fibrosis. *J Gastroenterol* 2012; **47:** 461–9.
29 Ferraioli G, Tinelli C, Dal Bello B, Zicchetti M, Filice G, Filice C. Accuracy of real-time shear wave elastography for assessing liver fibrosis in chronic hepatitis C: a pilot study. *Hepatology* 2012; **56:** 2125–33.